

University of New Orleans
ScholarWorks@UNO

Physics Faculty Publications

Department of Physics

2008

Dynamic and temperature effects in spin-transfer switching

Dorin Cimpoesu
University of New Orleans

Huy Pham
University of New Orleans

Leonard Spinu
University of New Orleans

Alexandru Stancu

Follow this and additional works at: https://scholarworks.uno.edu/phys_facpubs



Part of the [Physics Commons](#)

Recommended Citation

J. Appl. Phys. 104, 113918 (2008)

This Article is brought to you for free and open access by the Department of Physics at ScholarWorks@UNO. It has been accepted for inclusion in Physics Faculty Publications by an authorized administrator of ScholarWorks@UNO. For more information, please contact scholarworks@uno.edu.

Dynamic and temperature effects in spin-transfer switching

Dorin Cimpoesu,^{1,a)} Huy Pham,^{1,2} Alexandru Stancu,³ and Leonard Spinu^{1,2,b)}

¹Advanced Materials Research Institute, University of New Orleans, New Orleans, Louisiana 70148, USA

²Department of Physics, University of New Orleans, New Orleans, Louisiana 70148, USA

³Department of Physics, "Al. I. Cuza" University, Iasi 700506, Romania

(Received 5 August 2008; accepted 10 October 2008; published online 10 December 2008)

We have studied the dynamic switching triggered by spin angular momentum transfer in a pulsed current of a spin-valve-type trilayer structure, and its dependence on thermal effects. In order to determine the current pulse parameters, where fast and stable switching can be achieved, we have studied the magnetization's dynamics properties as a function of applied current pulse amplitude and shape, waiting time, and initial orientation, and also as a function of the Gilbert damping constant. The magnetic layer is assumed to be single domain, ellipsoid shaped. In this paper also we present the thermal fluctuation effects on the switching behavior. The model is based on the Landau–Lifshitz–Gilbert equation and the stochastic Landau–Lifshitz–Gilbert equation with a spin-transfer term included, which are numerically integrated. © 2008 American Institute of Physics.

[DOI: [10.1063/1.3032415](https://doi.org/10.1063/1.3032415)]

I. INTRODUCTION

The concept of spin angular momentum transfer torque proposed in 1996 by Slonczewski¹ and Berger² attracted an increased interest. In the presence of an electric current, a torque may act on the magnetization of a thin ferromagnetic layer, arising primarily from the transmission and reflection of incoming electrons. The spin-torque offers a new way to control the writing process in high density magnetic random access memory (MRAM) because a spin-polarized current can switch the magnetization of a ferromagnetic layer more efficiently than a current induced magnetic field. One year later, Slonczewsky proposed a spin-torque based magnetic memory,³ followed immediately by other ideas.^{4,5} Subsequently, it has been shown experimentally that spin transfer can indeed induce switching⁶ or microwave oscillations of the magnetization,^{7–9} and in 2005 a nonvolatile memory using a spin-torque magnetization switching was presented by Hosomi *et al.*,¹⁰ with a writing speed as high as 2 ns, and a write current as low as 200 μA . The technology using spin-torque effect is expected to increase the recording density of MRAM devices. Basically, the elementary spin-torque MRAM memory cell is a spin-valve-type trilayer structure, containing a thick pinned/fixed magnetic layer and a thin free magnetic layer, separated by a nonmagnetic metal spacer. A current becomes spin polarized after the electrons pass through the pinned layer. The spin-polarized electrons cross the nonmagnetic spacer and then, through conservation of angular momentum, place a torque on the free layer, which switches the orientation of the free layer's magnetization parallel to the pinned layer's magnetization. If a current of the opposite polarity is applied, the electrons pass first through the free layer and after crossing the nonmagnetic spacer, a torque is applied to the fixed layer. However, due to its larger thickness, the fixed layer does not switch. Simultaneously, a

fraction of the electrons will then reflect on the fixed layer and travel back across nonmagnetic spacer before interacting with the free layer. In this case the spin torque tends to align antiparallely the magnetizations of the two layers. This interaction due to spin-transfer is qualitatively different from the Ruderman–Kittel–Kasuya–Yosida exchange observed in the absence of the current, and also is different from the interaction with the magnetic field created by the current. In the simplest case such structure has two stable magnetic configurations, with the magnetizations of the two layers aligned parallel or antiparallel. A spin-transfer transmission mode⁴ or a spin-transfer reflection mode⁵ can be used to write the information.

Analytical and numerical simulations have shown that the magnetization reversal becomes very complicated when the spin-torque effect is taken into account, both using a macrospin model^{11–16} and a nonuniform magnetization model.^{17–20} Because the spin torque can increase or decrease the magnetic energy, stable precessional states can exist, and thus the magnetization will never converge to a final stable direction. Moreover, there are situations in a hysteresis loop when the magnetization increases with decreasing magnetic field. Thus, the analysis of thermal fluctuations in these systems is complicated because the self-oscillatory regions may exist in addition to stationary equilibrium states, and thermal fluctuations can induce switching between them. Since spin-transfer torque can pump a magnetic energy into the magnetic system, and thus the equilibrium temperature of the magnetic system is ill defined, in Ref. 21 an effective temperature and effective activation energy are introduced, based on a stationary solution of the Fokker–Planck equation. The numerical integration of the stochastic Landau–Lifshitz equation is used to support this theory. Using the Fokker–Planck rate calculation, Apalkov and Visscher²² showed that the spin-torque effect increases the Arrhenius factor in the switching rate, not by lowering the energy barrier, but by raising the effective spin temperature. An effective

^{a)}On leave from Department of Physics, "Al. I. Cuza" University, Iasi 700506, Romania. Electronic mail: cdorin@uaic.ro.

^{b)}Electronic mail: Lspinu@uno.edu.

tive potential barrier between a self-oscillatory regime and a stationary state, or between two oscillatory regimes, is defined in Ref. 23.

In Refs. 24–28 it is shown experimentally that the subnanosecond pulse durations leading to successful switching events are discrete durations reflecting the precessional nature of magnetization dynamics and the topological peculiarities in the set of possible magnetization trajectories. Flat plateaus alternating with rounded steps in the switching diagrams are explained taking into account the statistics of the possible initial states due to thermal fluctuations. The model developed in Ref. 27 assumes that the nonzero temperature results in a probabilistic distribution of the initial direction of the free layer's magnetization, already present when the current pulse is switched on, but that the temperature has no additional effect during the pulse application (i.e., during reversal).

An essential problem in the development of a device based on the spin-torque transfer is the evaluation of the minimum switching current that ensures a reliable magnetization reversal at high operating frequencies. Switching diagrams represented as current versus pulse duration plots²⁴ are very useful in finding optimum conditions for an error-free switching. In previous studies the influence of parameters as pulse amplitude, polarity and duration,²⁴ or bias hard axis fields²⁶ on switching diagrams were considered. With increasing demand for fast and low power nonvolatile memory devices, the influence of other variables on the switching diagrams must be considered. In this paper we present how the current sweep rate, damping constant, initial position, waiting time, and also the thermal fluctuations affect the switching, the reliability, and the writing speed of spin-torque devices. It will be shown that instead of a clear border between switching and nonswitching areas we have a layered transition region, with switching and nonswitching fringes, where the final state is sensitive to the pulse shape, duration, and amplitude, and also to thermal fluctuations. Our results show that this layered structure can be obtained at $T=0$ K, with no distribution of the initial states, as explained in Ref. 27, but only as an effect of the dynamics described by the Landau–Lifshitz–Gilbert (LLG) equation with a spin-transfer term included.^{1,2} We analyze also how the thermal fluctuations affect the switching behavior. The main goal is to determine the parameters of current pulse to achieve a fast and stable switching.

II. MODEL

In the absence of thermal fluctuations the dynamic behavior of the free layer's magnetization $\mathbf{M}=M_s\mathbf{m}$ ($M_s=|\mathbf{M}|$ being the saturation magnetization and assumed to be constant in magnitude) is described by the LLG equation with the spin-transfer term included,^{1,2}

$$\frac{d\mathbf{M}}{dt} = -|\gamma_0|\mathbf{M} \times \mathbf{H}_{\text{eff}} + \frac{\alpha}{M_s}\mathbf{M} \times \frac{d\mathbf{M}}{dt} + |\gamma_0|\frac{a_J}{M_s}\mathbf{M} \times (\mathbf{M} \times \mathbf{m}_p), \quad (1)$$

where $|\gamma_0|=2.211 \times 10^5$ (rad/s)/(A/m) is the gyromagnetic ratio, α is the Gilbert damping constant, \mathbf{H}_{eff} is the determin-

istic effective field which incorporates the applied field and the effects of different contributions to the free energy, the unit vector \mathbf{m}_p gives the direction of the spin polarization (direction of the fixed layer's magnetization), and the parameter a_J , which represents the strength of spin-transfer torque, is proportional to the current density as follows: $a_J = \hbar J_e / (2e|\mu_0 M_s d)$, where e is the electron charge, d is the thickness of the free layer, \hbar is the reduced Planck constant, and μ_0 is the vacuum permeability. The parameter a_J has the dimension of a magnetic field, and is positive when the electrons flow from the free into the fixed layer, stabilizing the antiparallel configuration. The applied current is perpendicular to the sample's plane, and it is assumed to carry a spin polarization parallel to the pinned layer's magnetization. We assume that the parameter a_J is independent of the orientation of free layer, the spin-transfer torque being proportional to the sine of the angle between \mathbf{m}_p and \mathbf{m} , namely, with $|\mathbf{m} \times (\mathbf{m} \times \mathbf{m}_p)|$ (i.e., the so-called sine approximation). The damping parameter is treated as a constant, even though there are theoretical and experimental evidences that α can be affected with various factors such as the magnetization's orientation^{29,30} and temperature.³¹ We also note that the validity of the Gilbert damping term in the presence of spin torque is being debated in literature.^{32,33} In our simulations the effective field consists only of demagnetizing field, no further anisotropy being considered. The magnetic field created by the applied current, and also the magnetostatic and exchange interactions between the two layers are neglected. Equation (1) can be equivalently written as

$$\frac{1 + \alpha^2}{|\gamma_0|} \frac{d\mathbf{M}}{dt} = -\mathbf{M} \times (\mathbf{H}_{\text{eff}} + \alpha a_J \mathbf{m}_p) - \frac{\alpha}{M_s} \mathbf{M} \times \left[\mathbf{M} \times \left(\mathbf{H}_{\text{eff}} - \frac{a_J}{\alpha} \mathbf{m}_p \right) \right], \quad (2)$$

where the first term on the right-hand side describes the gyromagnetic precession (conserving the energy), and the second term describes damping (dissipating energy and making the system relax to a local energy minimum). From Eq. (2) we observe that the spin torque is fundamentally different from the effective field and from damping, having both effects: it is a source of precessional motion as a magnetic field, and also can serve as damping/antidamping source. Due to this dual function of the spin torque the magnetization reversal becomes a very complicated issue even for a single domain (macrospin) model.

In the presence of thermal agitation it is supposed that the damping constant α describes in LLG equation only the statistical (ensemble) average of rapidly fluctuating random forces, and a stochastic thermal field \mathbf{H}_{th} should be added to the deterministic effective field \mathbf{H}_{eff} in Eqs. (1) and (2).³⁴ The stochastic field is assumed to be a Gaussian random process with a white spectrum,³⁴

$$\langle H_{\text{th},i}(t) \rangle = 0,$$

$$\langle H_{\text{th},i}(t) H_{\text{th},j}(t') \rangle = 2D \delta_{ij} \delta(t - t'),$$

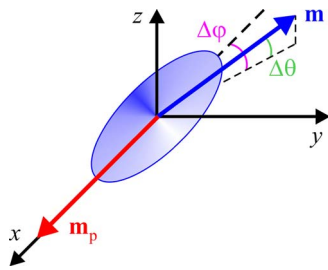


FIG. 1. (Color online) Schematic of the free layer, assumed to be ellipsoid shaped and single domain. The ellipsoid's principal axes are along the x , y , and z axes, with x and y in the plane of layer, and x along the longest axis. The axes' lengths are $2a=100$ nm, $2b=75$ nm, and thickness $d=2$ nm. The initial direction of the free layer's normalized magnetization \mathbf{m} is described by the angles $\Delta\theta$ and $\Delta\varphi$. The pinned ferromagnetic layer's normalized magnetization \mathbf{m}_p is held fixed at the direction of the free layer's long axis.

$$D = \frac{\alpha k_B T}{\gamma_0 \mu_0 M_s V},$$

where $\langle \rangle$ means the statistical average over different realizations of the fluctuating field, k_B is Boltzmann's constant, i and j are Cartesian indices, the Kronecker δ_{ij} expresses that the different components of \mathbf{H}_{th} are uncorrelated, and the Dirac δ expresses that $H_{th,i}(t)$ and $H_{th,j}(t')$ are correlated only for time intervals $t-t'$ much shorter than the time required for an appreciable change in \mathbf{M} . The constant D gives the strength of the thermal fluctuations, and it is determined from statistical-mechanical considerations.

We assume that solely the free layer is affected by thermal fluctuations, while \mathbf{m}_p does not change its direction. Also it is assumed that thermal fluctuations do not affect the spin-torque term a_j because the spin torque comes from the conduction electrons, whose transport properties are less affected by thermal fluctuations since the Fermi level is much higher than thermal energy. Besides, the fluctuating field is assumed independent of the spin torque. No temperature dependence of the anisotropy constant and saturation magnetization is taken. The stochastic field changes the deterministic motion of the magnetization into a random walk. The stochastic LLG (SLLG) equation is numerically integrated using an implicit midpoint time-integration technique.³⁵ The magnetic properties follow from an average over many numerical realizations of the dynamic process (discrete Brownian paths).

The free magnetic layer is assumed to be single domain, ellipsoid shaped, making the demagnetizing field uniform across the entire layer. The saturation magnetization $M_s = 12 \times 10^6 / 4\pi$ A/m was chosen. The ellipsoid's principal axes are taken along x , y , and z axes, respectively (see Fig. 1): long-axis length $2a=100$ nm (along Ox axis), short-axis length $2b=75$ nm (along Oy axis), and thickness $d=2$ nm, leading to demagnetizing factors $N_x=0.014$, $N_y=0.022$, and $N_z=0.964$, and accordingly, to demagnetizing fields: $\mu_0 H_{d,x} = \mu_0 N_x M_s = 16.93$ mT, $\mu_0 H_{d,y} = \mu_0 N_y M_s = 25.97$ mT, $\mu_0 H_{d,z} = \mu_0 N_z M_s = 1.157$ T, and to in-plane uniaxial shape anisotropy field $\mu_0 H_{sh} = \mu_0 (N_y - N_x) M_s = 9.04$ mT. Hereby we assume that the free layer has two contributions to anisotropy: an easy plane and an easy axis that is directed in this plane. In this way, in the absence of any applied magnetic field or

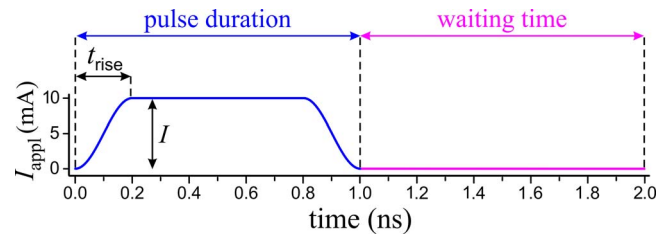


FIG. 2. (Color online) Time dependence of the applied current pulse. The sweep rate is defined as $v_j = I/t_{rise}$ and it is constant so that the rise/fall time is a function of pulse's amplitude. Unless otherwise specified, the final state of the magnetic moment is taken after a waiting time equal with the pulse duration.

electric current, the \mathbf{m} 's equilibrium orientations are along the $-x$ and $+x$ axes. By passing a current through spin-valve device one can switch \mathbf{m} back and forth between these two stable states. A current $I=1$ mA corresponds to a current density $J_e = I/\pi ab = 0.17 \times 10^8$ A/cm² and to $\mu_0 a_j = 29.27$ mT. The direction \mathbf{m}_p of the fixed layer's magnetization is taken along $+x$ direction so that the free layer's easy axis is parallel to the spin polarization of the electric current.

If initially the magnetic moments of fixed layer and free layer are aligned, there is no torque acting on the free layer. However, at finite temperature the thermal agitation assures that at no time this happens. In our simulations in the absence of thermal fluctuations, the initial direction of \mathbf{m} is described by the angles $\Delta\theta$ and $\Delta\varphi$, as shown in Fig. 1.

Because an instantaneous change in the applied current from zero to any other value is not very realistic, sinusoidal time dependence for the current pulse rise and fall are assumed (see Fig. 2). The rise/fall time is a function of the pulse's amplitude, so that the current sweep rate v_j , defined as the ratio between the amplitude and pulse's rise/fall time, is constant. Pulse duration is defined as the interval between the moment when current begins to increase, and the moment when the current comes back to zero. At a given temperature the switching properties are discussed as a function of applied current pulse amplitude, duration, and shape. Unless otherwise specified, the final state of the magnetic moment is taken after a time equal with the pulse duration, following pulse's termination.

III. RESULTS

A. Dynamic effects

Let us assume that before applying the current pulse, the free layer's magnetization is slightly tilted away from the $-x$ direction, into the xy plane, making a small angle $\Delta\varphi$ with the $-x$ axis (see Fig. 1). As it is shown by dynamical Eq. (2), the first term on the right-hand side pulls the magnetization vector away from the xy plane in the $+z$ direction, while the second term causes a movement into the direction of the $-x$ axis. The torque created by a negative current pulse (which stabilizes the parallel configuration) has an opposite effect: the precessional term pulls \mathbf{m} in the $-z$ direction, and the second term serves as an antidamping source, pushing \mathbf{m} in the opposite direction as demagnetizing field does, away from the $-x$ axis direction. The spin-torque term increases as the applied current increases. In some ranges of applied cur-

rent amplitude and duration, \mathbf{m} switches its orientation to become aligned with the spin polarization. As we see from this simple description, it is of paramount importance to take into account a current pulse with an increasing time, instead of a current applied infinitely abruptly (Heaviside step function). On the other hand, the magnetization reversal in a time dependent applied current is different from that in a constant current, making the magnetization dynamics quite complicated.

The damping α is not accurately known in a spin-valve system, and recent studies^{36–38} for ultrathin films show that α is enhanced when a nonmagnetic metal is deposited on a ferromagnetic film. Consequently, first we have studied the damping dependence of the spin-torque assisted switching.

For convenience, in all figures presented throughout this paper the absolute value of the applied current is used, while a negative current was used in simulations in order to switch from antiparallel (AP) to parallel (P) configuration.

The AP-P switching maps in the absence of thermal fluctuations ($T=0$ K), as a function of current pulse amplitude (from 0 to $I_{\max}=10$ mA) and duration (from $t_{\min}=I_{\max}/v_I$ to $t_{\max}=2$ ns), for a current sweep rate $v_I=1$ mA/ps, and different values of damping constant α are presented in Fig. 3(a). The minimum pulse duration t_{\min} is imposed by the condition to have a “pure” sinusoidal pulse for the maximum amplitude I_{\max} . Initially the magnetization of the free layer is in the film plane ($\Delta\theta=0$), making an angle $\Delta\varphi=10^{-3}$ deg with the direction of the pinned layer. The state of the magnetic moment is taken after a time equal with the pulse duration, following the pulse’s termination. From Fig. 3(a) we can see that the boundary which delimits the switching and nonswitching regions is not only a smooth hyperbola, it also has superimposed discrete features with a seashell spiral pattern or onionlike structure. In the seashell patterns the switching and nonswitching areas alternate with increasing current pulse amplitude and duration. When the pulse’s length is too short, a significant ringing of the magnetization still exists during the current pulse and the final state is determined by the position of the magnetization at the end of the pulse. Consequently, the layered structure predominates for short current pulses.

An increase in α diminishes the layered structure of the switching diagrams, giving rise to a clearer separation between the nonswitching/switching regions, but decreases the area of the stable switching region, i.e., a higher amplitude or longer pulse is needed to switch the magnetization. An increase in α increases the energy dissipation rate [see Eq. (2)] and in this way diminishes the ringing of the magnetization. The positions of the seashell spiral patterns are changing with the increase in α , shifting toward higher values of the current amplitude.

On a log-log scale the border between switching and nonswitching regions is almost a straight line, with seashell spiral patterns superimposed [see Fig. 3(b)]. An increase in α decreases the straight line’s inclination and changes also its position, decreasing the extent of switching region. The straight line border illustrates that the switching requires a pulse duration that scales with the inverse of the current

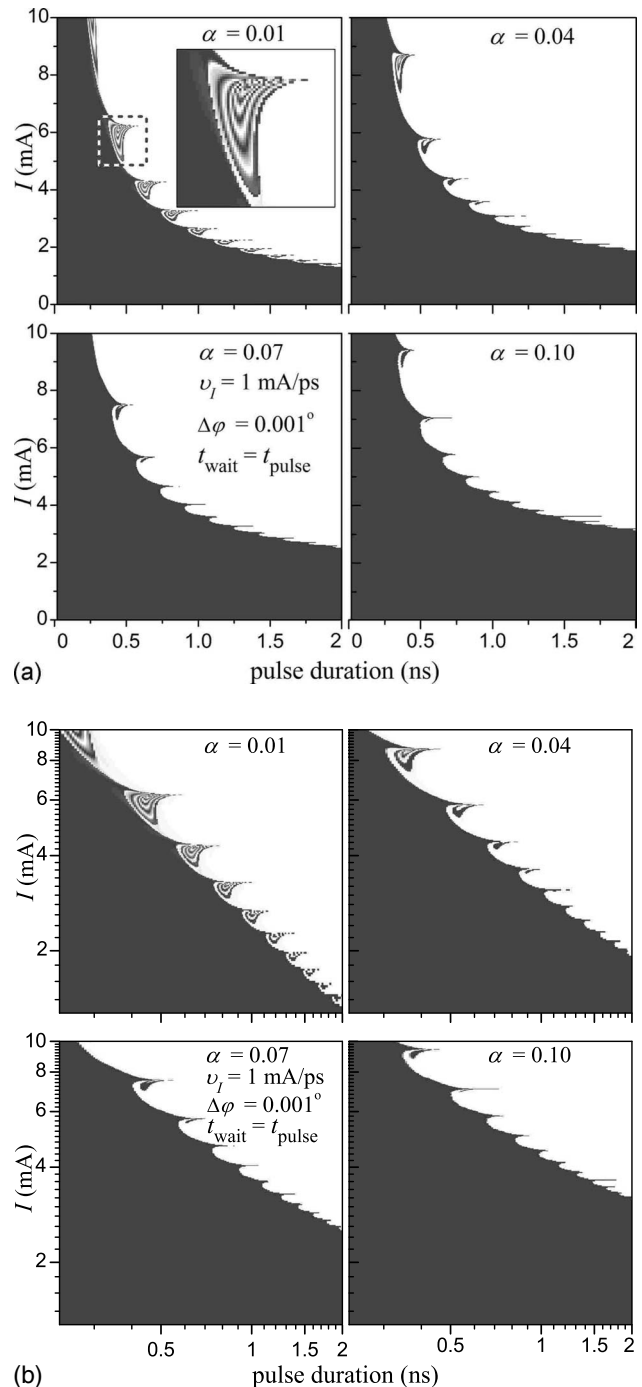


FIG. 3. (a) AP-P switching diagrams at $T=0$ K, as a function of current pulse amplitude and duration, for a current sweep rate $v_I=1$ mA/ps, and different values of damping constant α . Initially the magnetization of the free layer is in the film plane ($\Delta\theta=0$), making an angle $\Delta\varphi=10^{-3}$ deg with the direction of the fixed layer. Black areas represent $m_x=-1$ (where m_x is the \mathbf{m} 's projection on the x axis), white areas represent $m_x=1$, and the intermediate values of m_x are represented with shades of gray. The state of the magnetic moment is taken after a time equal with the pulse duration, following the pulse’s termination. The inset (top left) shows a zooming into a portion of the border between stable switching and nonswitching zones. (b) Same as (a) but on a log-log scale.

pulse amplitude, recalling the result of Sun from Ref. 11. Further in this paper the Gilbert damping is kept constant, and a value $\alpha=0.01$ is used.

For $\alpha=0.01$ the magnetization vector is still ringing after a waiting time equal with pulse duration, and consequently

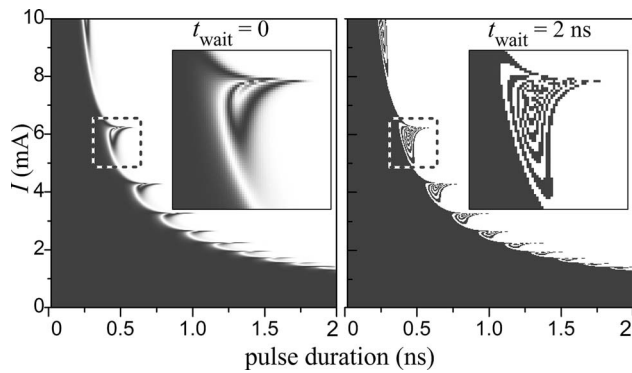


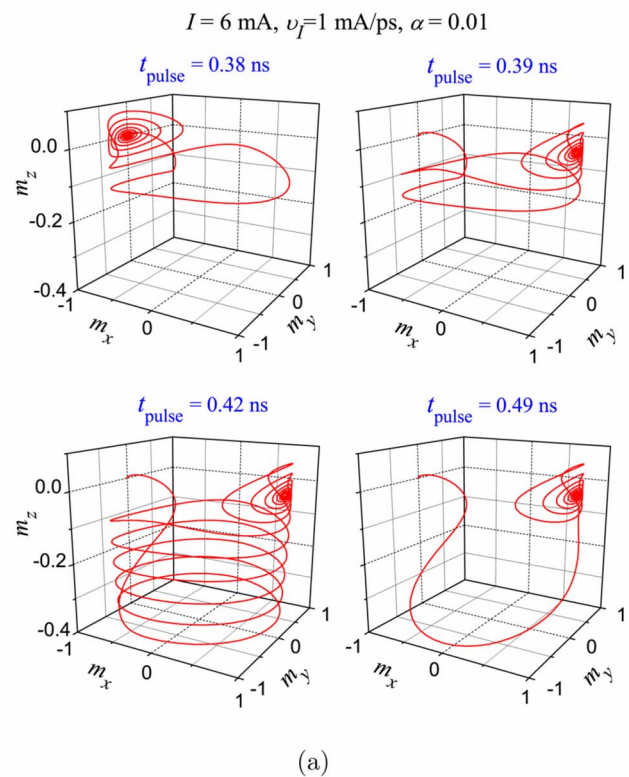
FIG. 4. AP-P switching diagrams at $T=0$ K for a current sweep rate $v_j = 1$ mA/ps, damping constant $\alpha=0.01$, the state of the magnetic moment being taken after a waiting time $t_{\text{wait}}=0$ (left) and $t_{\text{wait}}=2$ ns (right), respectively, after pulses' termination.

in the corresponding diagram the magnetization is not only along the $-x$ or $+x$ axis in the border region, but can take any other direction, shown in Fig. 3 with shades of gray. If some states of intermediate orientation are created by a given pulse, these states will relax to either parallel or antiparallel state, along easy axis, after a sufficient long time, as we can see in the right panel of Fig. 4, where the switching diagram is built using the magnetization's orientation after a waiting time $t_{\text{wait}}=2$ ns, when the magnetization's ringing almost vanishes and \mathbf{m} is either along the $-x$ or $+x$ axis. The seashell spiral pattern of the diagram persists even a long time after the current pulse is cut off, this being a signature of dynamical effects in spin-torque switching. Also, it exists when the current is cut off (see left panel in Fig. 4) and evolves in time into a more intricate structure (see right panel in Fig. 4).

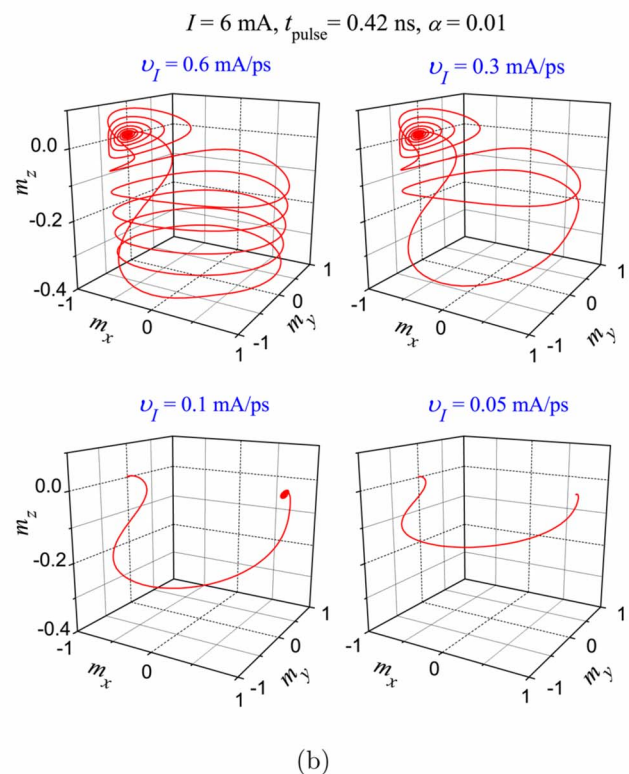
Because no interaction has been taken between the pinned and free layers, the P-AP switching diagrams are similar, only the sign of m_x being reversed. All the results presented in this paper are obtained when a current pulse is applied to a spin valve in the AP state.

Flat plateaus alternating with rounded steps in experimental switching diagrams were reported by Devolder *et al.* in Ref. 27 and they were explained by taking into account the statistics of the possible initial states due to thermal fluctuations. However, our results show that a seashell spiral pattern can be obtained in the absence of thermal fluctuations, i.e., at $T=0$ K, with no distribution of the initial states, only as an effect of the dynamics described by the LLG equation with a spin-transfer term included. The reported pulse durations in Ref. 27 are from 1 to 10 ns (full width at half maximum), with a rise time of 55 ps, a maximum current of 20 mA, and a 1 nm thick CoFe free layer, etched into 75×150 and 75×113 nm² elongated hexagons, respectively.

From Figs. 3 and 4 we can see that in the border region the final state is sensitive to the pulse duration and amplitude. However also the precession of the magnetization is very sensitive to these parameters, as we can see in Fig. 5. In the first case from Fig. 5(a) one observes that the magnetic moment can cross the energy barrier, from -1 to $+1$, followed by a return to the initial state, while in the second and



(a)



(b)

FIG. 5. (Color online) The precession of magnetization \mathbf{m} under the influence of a current pulse with $I=6$ mA. (a) For $v_j=1$ mA/ps, and different values of the pulse duration: $t_{\text{pulse}}=0.38, 0.39, 0.42,$ and 0.49 ns; (b) for $t_{\text{pulse}}=0.42$ ns, and different values of the current sweep rates $v_j=0.6, 0.3, 0.1,$ and 0.05 mA/ps. Initially \mathbf{m} is in the film plane, making an angle $\Delta\varphi = 10^{-3}$ deg with \mathbf{m}_p . The damping constant $\alpha=0.01$.

third cases the magnetic moment oscillates many times between -1 and $+1$, the magnetization finally relaxing to the reverse easy axis position $m_x=+1$. We observe not only

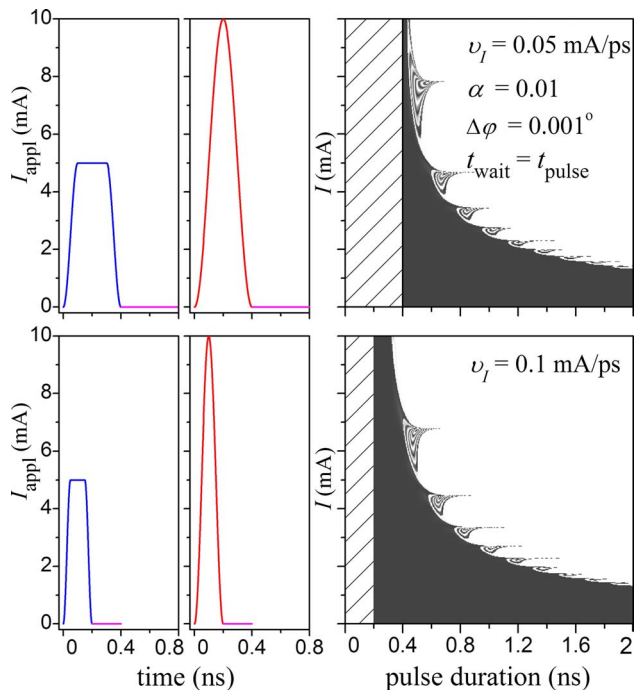


FIG. 6. (Color online) AP-P switching diagrams at $T=0$ K for a current sweep rate $v_l=0.05$ mA/ps (up right), and $v_l=0.1$ mA/ps (down right), respectively, for a damping constant $\alpha=0.01$. In the hatched zones no current pulses are applied. In the left panels the applied current pulses corresponding to minimum pulse duration $t_{\min}=I_{\max}/v_l$ for $I_{\max}=5$ mA and $I_{\max}=10$ mA, respectively, are presented. For $I_{\max}=10$ mA the pulse is pure sinusoidal.

an in-plane dynamics of the magnetic moment but also a significant out-of-plane component (z direction) during the oscillation. However, we note that not all three axes are equal in Fig. 5, namely, that the z axis is from -0.4 to $+0.1$, while the x and y axes are from -1 to $+1$. Thus, current pulses with the same amplitude but different duration have not only different switching outcomes but also very different precession trajectories. Decreasing the pulse's sweep rate, namely, increasing the pulse's rising time, the out-of-plane movement of the magnetization diminishes, and also the ringing diminishes [see Fig. 5(b)]. For a fast and reliable switching, such ringing must be avoided, as the damping time can take several nanoseconds. The ringing may be diminished using a relatively slow rise time pulse [see Fig. 5(b), where in the last case a ballistic trajectory is obtained].

However even diminishing the sweep rate, the switching properties are dominated by the details of the magnetization's precession, and a layerlike structure of switching diagram has been obtained also for $v_l=0.05$ mA/ps (see Fig. 6). Decreasing the sweep rate also diminishes the region of stable switching (white region in switching diagram).

In Ref. 27 the switching duration is defined as the instant of time when the hard axis is overcome, i.e., when the condition $m_x=0$ is fulfilled. However, from Fig. 5 we can see that the magnetization can undergo many precessions between AP and P states, overcoming the hard axis several times, with different final states, depending on many factors, such as damping constant, current pulse's shape, or duration.

In all the results presented until now the initial direction of \mathbf{m} was considered in the layer's plane, making an angle

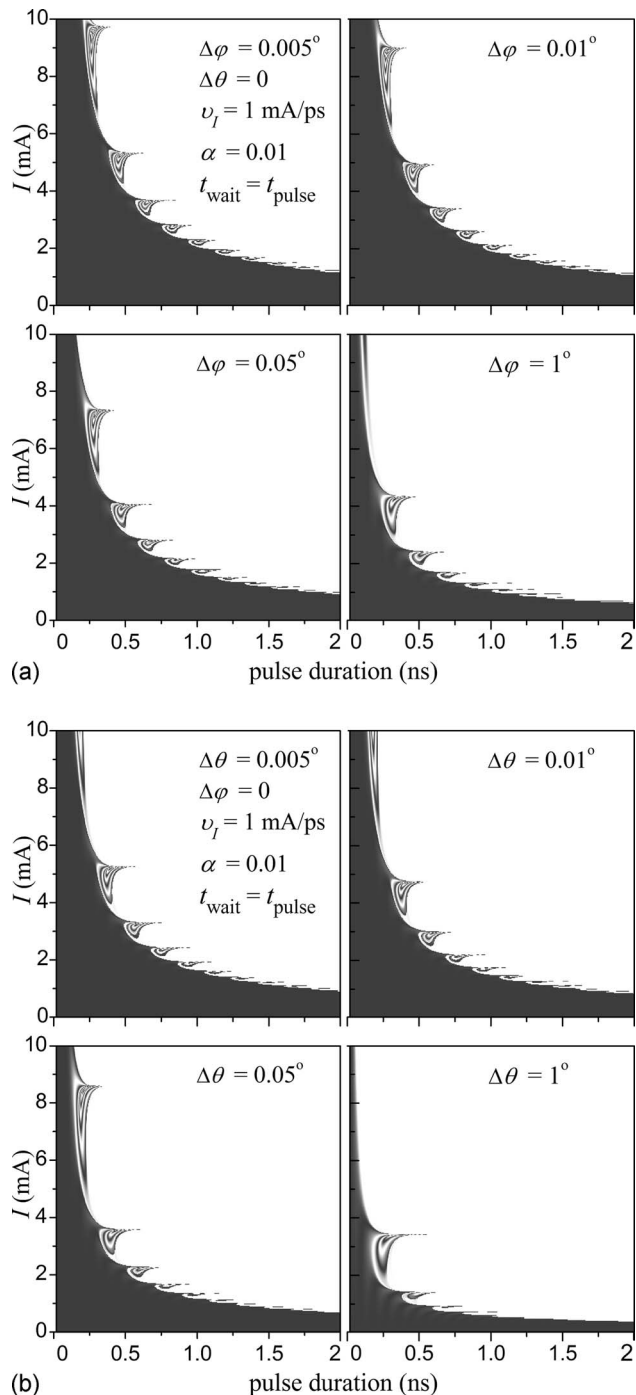


FIG. 7. AP-P switching diagrams at $T=0$ K for a current sweep rate $v_l=1$ mA/ps, a damping constant $\alpha=0.01$: (a) for different initial orientations $\Delta\varphi$ of magnetization \mathbf{m} in the layer's plane, and (b) for different out-of-plane initial orientations $\Delta\theta$ of magnetization \mathbf{m} .

$\Delta\varphi=10^{-3}$ deg with the direction \mathbf{m}_p of the fixed layer. Increasing the offset angle $\Delta\varphi$, the switching region increases, and still there are fringes at the border between switching and nonswitching areas [see Fig. 7(a)]. For the same value, a deviation $\Delta\theta$ out of plane has a bigger effect than the in-plane deviation $\Delta\varphi$ [see Figs. 7(a) and 7(b)].

B. Temperature effects

The effect of spin-transfer torque is significant for magnetic particles of small dimensions, typically few tens of na-

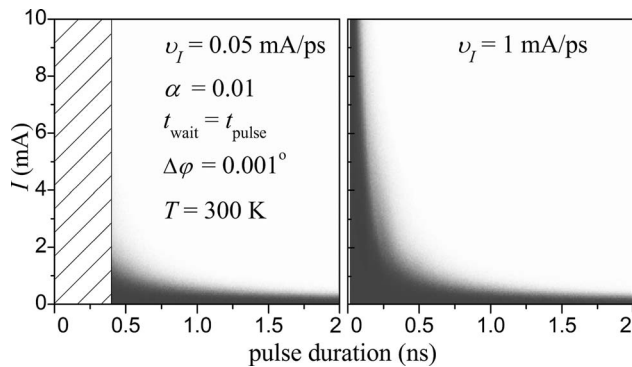


FIG. 8. AP-P switching diagrams at $T=300$ K for a current sweep rate $v_l = 0.05$ mA/ps (left) and $v_l = 1$ mA/ps (right), respectively, for a damping constant $\alpha=0.01$.

nometers. For such small dimensions the high-frequency magnetic noise due to the thermal fluctuations may pose a fundamental limitation to the device performance, significantly influencing the magnetization's dynamics and switching. The magnetic moments have thermally activated random oscillations close to the bottom of the energy minima. This type of oscillations can be induced over a finite energy barrier, as well. In the presence of thermal fluctuations, identical pulses do or do not switch the magnetization, with a certain probability. The probability of switching is plotted in a gray coded diagram as a function of current pulse amplitude and duration in Fig. 8 for two values of the current sweep rate. Each simulated point from diagrams represents the statistic of 1024 repeatedly writing operations at certain pulse amplitude and duration. We can see that temperature increases the switching area, and that instead of a clear border between switching and non-switching areas we have a transition region where the final state is sensitive to thermal fluctuations.

IV. CONCLUSIONS

Based on the magnetization vector dynamics, as described by the LLG/SLLG equation of motion, the switching properties of a spin-valve-type trilayer structure have been presented. We have shown that in the switching diagrams the boundary, which delimits the stable switching and non-switching regions, is not smooth but it has a seashell spiral pattern (fringes), with switching and non-switching areas alternating with increasing current pulse amplitude and duration. These fringes exist when the current is cut off and evolve in time into a more intricate structure. When the pulse length is too short, a significant ringing of the magnetization still exists during the current pulse and the final state is determined by the position of the magnetization at the end of the pulse. For a fast and reliable switching such ringing must be avoided, as the damping time can take several nanoseconds. The ringing may be diminished, for example, using a relatively slow rise time pulse. Also, we have presented how the thermal fluctuations affect the switching behavior.

ACKNOWLEDGMENTS

Work at AMRI was supported by the DARPA under Grant No. HR0011-07-1-0031. Calculations were performed on computational facilities provided by Louisiana Optical Network Initiative (<http://www.loni.org>) which was supported by the Louisiana Board of Regents. This work was partially supported by Romanian CNCSIS under the Grant A(RELSWITCH).

- ¹J. C. Slonczewski, *J. Magn. Magn. Mater.* **159**, L1 (1996).
- ²L. Berger, *Phys. Rev. B* **54**, 9353 (1996).
- ³J. C. Slonczewski, U.S. Patent No. 5,695,864 (9 December 1997).
- ⁴Y. Huai and P. P. Nguyen, U.S. Patent No. 6,920,063 B2 (19 July 2005).
- ⁵F. B. Mancoff, B. N. Engel, and N. D. Rizzo, U.S. Patent No. 7,149,106 B2 (12 December 2006).
- ⁶E. B. Myers, D. C. Ralph, J. A. Katine, R. N. Louie, and R. A. Buhrman, *Science* **285**, 867 (1999).
- ⁷W. Weber, S. Riesen, and H. C. Siegmann, *Science* **291**, 1015 (2001).
- ⁸S. I. Kiselev, J. C. Sankey, I. N. Krivorotov, N. C. Emley, R. J. Schoelkopf, R. A. Buhrman, and D. C. Ralph, *Nature (London)* **425**, 380 (2003).
- ⁹I. N. Krivorotov, N. C. Emley, J. C. Sankey, S. I. Kiselev, D. C. Ralph, and R. A. Buhrman, *Science* **307**, 228 (2005).
- ¹⁰M. Hosomi, H. Yamagishi, T. Yamamoto, K. Bessho, Y. Higo, K. Yamane, H. Yamada, M. Shoji, H. Hachino, C. Fukumoto, H. Nagao, and H. Kano, *Tech. Dig. - Int. Electron Devices Meet.* **2005**, 459.
- ¹¹J. Z. Sun, *Phys. Rev. B* **62**, 570 (2000).
- ¹²J. Z. Sun, *IBM J. Res. Dev.* **50**, 81 (2006).
- ¹³J. Xiao, A. Zangwill, and M. D. Stiles, *Phys. Rev. B* **72**, 014446 (2005).
- ¹⁴Ya. B. Bazaliy, B. A. Jones, and S. C. Zhang, *Phys. Rev. B* **69**, 094421 (2004).
- ¹⁵H. Morise and S. Nakamura, *Phys. Rev. B* **71**, 014439 (2005).
- ¹⁶G. Bertotti, C. Serpico, I. D. Mayergoyz, A. Magni, M. d'Aquino, and R. Bonin, *Phys. Rev. Lett.* **94**, 127206 (2005).
- ¹⁷J. Miltat, G. Albuquerque, A. Thiaville, and C. Vouille, *J. Appl. Phys.* **89**, 6982 (2001).
- ¹⁸D. V. Berkov and N. L. Gorn, *Phys. Rev. B* **71**, 052403 (2005).
- ¹⁹D. V. Berkov and N. L. Gorn, *Phys. Rev. B* **72**, 094401 (2005).
- ²⁰Z. Li and S. Zhang, *Phys. Rev. B* **68**, 024404 (2003).
- ²¹Z. Li and S. Zhang, *Phys. Rev. B* **69**, 134416 (2004).
- ²²D. M. Apalkov and P. B. Visscher, *Phys. Rev. B* **72**, 180405 (2005).
- ²³C. Serpico, G. Bertotti, I. D. Mayergoyz, M. d'Aquino, and R. Bonin, *J. Appl. Phys.* **99**, 08G505 (2006).
- ²⁴A. A. Tulapurkar, T. Devolder, K. Yagami, P. Crozat, C. Chappert, A. Fukushima, and Y. Suzuki, *Appl. Phys. Lett.* **85**, 5358 (2004).
- ²⁵T. Devolder, A. Tulapurkar, Y. Suzuki, C. Chappert, P. Crozat, and K. Yagami, *J. Appl. Phys.* **98**, 053904 (2005).
- ²⁶T. Devolder, P. Crozat, J.-V. Kim, C. Chappert, K. Ito, J. A. Katine, and M. J. Carey, *Appl. Phys. Lett.* **88**, 152502 (2006).
- ²⁷T. Devolder, C. Chappert, J. A. Katine, M. J. Carey, and K. Ito, *Phys. Rev. B* **75**, 064402 (2007).
- ²⁸T. Devolder, C. Chappert, and K. Ito, *Phys. Rev. B* **75**, 224430 (2007).
- ²⁹C. E. Patton, *J. Appl. Phys.* **39**, 3060 (1968).
- ³⁰R. D. McMichael, M. D. Stiles, P. J. Chen, and W. F. Egelhoff, Jr., *J. Appl. Phys.* **83**, 7037 (1998).
- ³¹C. D. Stanciu, A. V. Kimel, F. Hansteen, A. Tsukamoto, A. Itoh, A. Kirilyuk, and Th. Rasing, *Phys. Rev. B* **73**, 220402(R) (2006).
- ³²M. D. Stiles, W. M. Saslow, M. J. Donahue, and A. Zangwill, *Phys. Rev. B* **75**, 214423 (2007).
- ³³N. Smith, arXiv:0706.1736v1.
- ³⁴W. F. Brown, Jr., *Phys. Rev.* **130**, 1677 (1963).
- ³⁵M. d'Aquino, C. Serpico, G. Coppola, I. D. Mayergoyz, and G. Bertotti, *J. Appl. Phys.* **99**, 08B905 (2006).
- ³⁶R. Urban, G. Woltersdorf, and B. Heinrich, *Phys. Rev. Lett.* **87**, 217204 (2001).
- ³⁷Y. Tserkovnyak, A. Brataas, and G. E. W. Bauer, *Phys. Rev. Lett.* **88**, 117601 (2002).
- ³⁸P. M. Braganca, I. N. Krivorotov, O. Ozatay, A. G. F. Garcia, N. C. Emley, J. C. Sankey, D. C. Ralph, and R. A. Buhrman, *Appl. Phys. Lett.* **87**, 112507 (2005).